Electroweak corrections to Higgs boson decays to $\gamma\gamma$ and W^+W^- in standard model EFT

S. Dawson and P. P. Giardino

Department of Physics, Brookhaven National Laboratory, Upton, New York 11973, USA

(Received 3 August 2018; published 5 November 2018)

Higgs decays to gauge boson pairs are a crucial ingredient in the study of Higgs properties, with the decay $H \to \gamma\gamma$ being particularly sensitive to new physics effects. Assuming all potential new physics occurs at energies far above the weak scale, deviations from standard model predictions can be parametrized in terms of the coefficients of a standard model effective field theory (SMEFT). When experimental limits on the SMEFT coefficients reach an accuracy of a few percent, predictions must be done beyond the lowest order in the SMEFT in order to match theory and experimental accuracy. This paper completes a program of computing the one-loop electroweak SMEFT corrections to $H \to VV'$, $V = W^{\pm}, Z, \gamma$. The calculation of the real contribution to $H \to W^+W^-\gamma$ is performed by mapping two-loop amplitudes to the three-body phase space.

DOI: 10.1103/PhysRevD.98.095005

I. INTRODUCTION

The LHC Higgs program is entering an era of precision measurements that requires a program of higher order theoretical calculations. The need for precise calculations is driven by (1) the nondiscovery of new particles that implies that the scale of beyond the standard model (BSM) physics must typically be much higher than ~1 TeV and (2) the anticipated precision in the Higgs measurements at the high luminosity LHC [1,2]. In order to study deviations of Higgs properties from the SM predictions, a consistent theoretical framework is needed so that the accuracy of theoretical calculations is comparable to that of the measurements.

The standard model (SM) QCD and electroweak contributions to Higgs production and decay are known to at least next to leading order (NLO) for all relevant processes and provide a framework for comparison [3]. In the LHC Run-1, deviations of Higgs measurements from SM predictions were typically expressed in terms of limits on coupling constant modifiers [4]. This κ approach rescales all Higgs couplings by constant factors and is not sensitive to kinematic distributions. As measurements approach the level of 5%–10% accuracy, however, it becomes necessary to include electroweak corrections to the predictions, which in turn necessitates the use of effective field theory techniques, since electroweak corrections typically cannot be incorporated into a simple rescaling of the Higgs couplings.

The use of effective field theories for studying Higgs production and decay is well established [5–7]. The SM effective field theory (SMEFT) assumes that the Higgs is an $SU(2)_L$ doublet and parametrizes new physics through an expansion in higher dimensional operators,

$$\mathcal{L} = \mathcal{L}_{\rm SM} + \Sigma_{k=5}^{\infty}\Sigma_{i=1}^{n}\frac{\mathcal{C}_i^k}{\Lambda^{k-4}}O_i^k, \tag{1}$$

where the $SU(3) \times SU(2)_L \times U(1)_Y$ invariant dimension-k operators are constructed from SM fields and all of the BSM physics effects reside in the coefficient functions, $\mathcal{C}_i^k$. If the scale $\Lambda \gg v$, then it suffices to truncate the expansion at dimension 6. This large separation of scales is necessary in order for a study containing only dimension-6 operators to be valid, since the effects of the dimension-8 operators are assumed to be suppressed by an additional factor of v^2/Λ^2 and are neglected. Similarly, it is assumed that there are no new particles in the theory at scales below Λ.

We need predictions to NLO QCD and EW accuracy in the SMEFT so that the theoretical predictions have roughly the same uncertainties as the experimental results. For processes with strong interactions, many NLO QCD results in the SMEFT exist, particularly in the top-Higgs sector [8]. Electroweak corrections in the SMEFT [9] are available for only a handful of processes: $H \to b\bar{b}$ [10,11], $H \to \gamma\gamma$ [9,12–14], $H \to Z\gamma$ [15] and $Z \to f\bar{f}$ [16]. Here, we complete the program of computing the on-shell decays $H \to VV'$, $(V = Z,\ W^{\pm},\ \gamma)$, at one loop in the SMEFT. Previously, we presented one-loop SMEFT results for $H \to Z\gamma$ and for the (unphysical) on-shell decay $H \to ZZ$ and [15].

TABLE I. Dimension-6 operators relevant for the one-loop contributions to $H \to VV$ ($V = W, Z, \gamma$) (from [20]). For brevity we suppress fermion chiral indices L, R. $I = 1, 2, 3$ is an $SU(2)$ index; p, r are flavor indices; and $\phi^\dagger i\overleftrightarrow{D}_\mu \phi \equiv \phi^\dagger D_\mu \phi - (D_\mu \phi^\dagger)\phi$.

$\mathcal{O}_W$	$\epsilon^{IJK} W_\mu^{I\nu} W_\nu^{J\rho} W_\rho^{K\mu}$	$\mathcal{O}_{\phi\Box}$	$(\phi^\dagger\phi)\Box(\phi^\dagger\phi)$	$\mathcal{O}_{\phi D}$	$(\phi^\dagger D^\mu \phi)^*(\phi^\dagger D_\mu \phi)$
$\mathcal{O}_{\substack{u\phi \\ p,r}}$	$(\phi^\dagger\phi)(\bar{q}'_p u'_r \tilde{\phi})$	$\mathcal{O}_{\phi W}$	$(\phi^\dagger\phi) W_{\mu\nu} W^{\mu\nu}$	$\mathcal{O}_{\phi B}$	$(\phi^\dagger\phi) B_{\mu\nu} B^{\mu\nu}$
$\mathcal{O}_{\phi WB}$	$(\phi^\dagger \tau^I \phi) W^I_{\mu\nu} B^{\mu\nu}$	$\mathcal{O}_{uW}$	$(\bar{q}'_p \sigma^{\mu\nu} u'_r)\tau^I \tilde{\phi} W^I_{\mu\nu}$	$\mathcal{O}_{\substack{uB \\ p,r}}$	$(\bar{q}'_p \sigma^{\mu\nu} u'_r)\tilde{\phi} B_{\mu\nu}$
$\mathcal{O}^{(3)}_{\substack{\phi l \\ p,r}}$	$(\phi^\dagger i\overleftrightarrow{D}^I_\mu \phi)(\bar{l}'_p \tau^I \gamma^\mu l'_r)$	$\mathcal{O}_{\substack{ll \\ p,r,s,t}}$	$(\bar{l}'_p \gamma_\mu l'_r)(\bar{l}'_s \gamma^\mu l'_t)$		

In this paper, we present the one-loop SMEFT results for $H \to \gamma\gamma$ and the on-shell process $H \to W^+W^-$. The result for the decay $H \to \gamma\gamma$ follows from the results of Ref. [15] and we compare with the results[1] of Refs. [12–14]. We consider two different input parameter choices in order to assess their numerical significance. Our result contains the full (constant plus logarithmic terms) SMEFT result for the renormalization of G_F.[2] Our one-loop $H \to W^+W^-$ result is an intermediate step on the way to the physical process $H \to W^+W^- \to 4$ fermions. The calculation of the real contributions from $H \to W^+W^-\gamma$ is performed using a mapping of the three-body phase space to two-loop amplitudes, which is of technical interest [18].

Section II reviews the one-loop electroweak renormalization for $H \to VV$ decays, Sec. III has results for $H \to W^+W^-$, and Sec. IV contains the one-loop results for $H \to \gamma\gamma$. Conclusions are contained in Sec. V.

II. BASICS

We use the Warsaw basis [19,20] where the relevant operators for the one-loop contributions to the decays $H \to VV$ are given in Table I and the Feynman rules and conventions in R_ξ gauge are taken from Ref. [21]. For simplicity, we assume a diagonal flavor structure for the coefficients $\mathcal{C}$, i.e., $\underset{p,r}{\mathcal{C}_i} = \mathcal{C}_i \underset{p,r}{\mathbb{1}}$, where p, r are flavor indices. Furthermore, we assume $\underset{e,\mu,\mu,e}{\mathcal{C}_{ll}} = \underset{\mu,e,e\mu}{\mathcal{C}_{ll}} \equiv \mathcal{C}_{ll}$ and $\underset{\mu,\mu,t,t}{\mathcal{C}^{(3)}_{lq}} = \underset{e,e,t,t}{\mathcal{C}^{(3)}_{lq}} \equiv \mathcal{C}^{(3)}_{lq}$.

The Higgs Lagrangian is

$$\begin{aligned}\mathcal{L} = {} & (D_\mu\phi)^\dagger(D_\mu\phi) + \mu^2\phi^\dagger\phi - \lambda(\phi^\dagger\phi)^2 \\ & + \frac{1}{\Lambda^2}(\mathcal{C}_\phi(\phi^\dagger\phi)^3 + \mathcal{C}_{\phi\Box}(\phi^\dagger\phi)\Box(\phi^\dagger\phi) \\ & + \mathcal{C}_{\phi D}(\phi^\dagger D_\mu\phi)^*(\phi^\dagger D_\mu\phi)),\end{aligned} \tag{2}$$

where ϕ is the usual Higgs doublet,

$$\phi = \begin{pmatrix} \phi^+ \\ \frac{1}{\sqrt{2}}(v + H + i\phi^0) \end{pmatrix}, \tag{3}$$

and v is the vacuum expectation value (VEV) defined as the minimum of the potential,

$$v \equiv \sqrt{2}\langle\phi\rangle = \sqrt{\frac{\mu^2}{\lambda}} + \frac{3\mu^3}{8\lambda^{5/2}}\frac{\mathcal{C}_\phi}{\Lambda^2}. \tag{4}$$

The Higgs kinetic terms in the resulting Lagrangian are not canonically normalized due to $\mathcal{O}_{\phi\Box}$ and $\mathcal{O}_{\phi D}$. As a consequence we need to shift the fields:

$$\begin{aligned} H &\to H\left(1 - \frac{v^2}{\Lambda^2}\left(\frac{1}{4}\mathcal{C}_{\phi D} - \mathcal{C}_{\phi\Box}\right)\right) \\ \phi^0 &\to \phi^0\left(1 - \frac{v^2}{\Lambda^2}\left(\frac{1}{4}\mathcal{C}_{\phi D}\right)\right) \\ \phi^+ &\to \phi^+. \end{aligned} \tag{5}$$

The physical mass of the Higgs to $\mathcal{O}(\frac{1}{\Lambda^2})$ becomes

$$M_H^2 = 2\lambda v^2 - \frac{v^4}{\Lambda^2}(3\mathcal{C}_\phi - 4\lambda\mathcal{C}_{\phi\Box} + \lambda\mathcal{C}_{\phi D}). \tag{6}$$

The SMEFT interactions also cause the gauge field kinetic energies to have noncanonical normalizations and following Ref. [21], we define "barred" fields and couplings,

$$\begin{aligned} \overline{W}_\mu &\equiv (1 - \mathcal{C}_{\phi W} v^2/\Lambda^2) W_\mu \\ \overline{B}_\mu &\equiv (1 - \mathcal{C}_{\phi B} v^2/\Lambda^2) B_\mu \\ \bar{g}_2 &\equiv (1 + \mathcal{C}_{\phi W} v^2/\Lambda^2) g_2 \\ \bar{g}_1 &\equiv (1 + \mathcal{C}_{\phi B} v^2/\Lambda^2) g_1 \end{aligned} \tag{7}$$

such that $\overline{W}_\mu \bar{g}_2 = W_\mu g_2$ and $\overline{B}_\mu \bar{g}_1 = B_\mu g_1$. The barred fields defined in this way have properly normalized kinetic energy terms. The masses of the W and Z fields to $\mathcal{O}(\frac{1}{\Lambda^2})$ are [21,22]

[1] The corrections due to the top loops in the SMEFT have been studied also in [17].

[2] References [9,12,13] contain only the logarithmic contributions to the SMEFT renormalization of G_F.

$$M_W^2 = \frac{\bar{g}_2^2 v^2}{4},$$
$$M_Z^2 = \frac{(\bar{g}_1^2+\bar{g}_2^2)v^2}{4} + \frac{v^4}{\Lambda^2}\left(\frac{1}{8}(\bar{g}_1^2+\bar{g}_2^2)\mathcal{C}_{\phi D} + \frac{1}{2}\bar{g}_1\bar{g}_2\mathcal{C}_{\phi WB}\right). \tag{8}$$

Dimension-6 four-fermion operators give contributions to the decay of the μ, changing the relation between the VEV, v, and the Fermi constant G_μ. Considering only contributions that interfere with the SM amplitude, we obtain the tree level result,

$$G_\mu \equiv \frac{1}{\sqrt{2}v^2} - \frac{1}{\sqrt{2}\Lambda^2}\mathcal{C}_{ll} + \frac{\sqrt{2}}{\Lambda^2}\mathcal{C}_{\phi l}^{(3)}, \tag{9}$$

where we assume the $\mathcal{C}_i$ are flavor universal. The tadpole counterterms are defined such that they cancel completely the tadpole graphs [23]. This condition identifies the renormalized vacuum as the minimum of the renormalized scalar potential at each order of perturbation theory.

Since the SMEFT theory is only renormalizable order by order in the (v^2/Λ^2) expansion, we drop all terms proportional to $(v^2/\Lambda^2)^a$ with $a > 1$. The one-loop SMEFT calculations contain both tree level and one-loop contributions from the dimension-6 operators, along with the full electroweak one-loop SM amplitudes.

We use a modified on-shell (OS) scheme, where the SM parameters are OS quantities. Since the coefficients of the dimension-6 operators are not physical observables, we treat them as $\overline{\text{MS}}$ parameters, so the renormalized coefficients are $\mathcal{C}(\mu) = \mathcal{C}_0 - \text{poles}$, where $\mathcal{C}_0$ are the bare quantities. The poles of the coefficients $\mathcal{C}_0$ are found from the renormalization group (RG) evolution of the coefficients computed in the unbroken phase of the theory in Refs. [22,24,25],

$$\mathcal{C}_i(\mu) = \mathcal{C}_{0,i} - \frac{1}{2\hat{\epsilon}}\frac{1}{16\pi^2}\gamma_{ij}\mathcal{C}_j, \tag{10}$$

where μ is the renormalization scale, γ_{ij} is the one-loop anomalous dimension,

$$\mu\frac{d\mathcal{C}_i}{d\mu} = \frac{1}{16\pi^2}\gamma_{ij}\mathcal{C}_j, \tag{11}$$

and $\hat{\epsilon}^{-1} \equiv \epsilon^{-1} - \gamma_E + \log(4\pi)$. At one loop, tree level parameters (denoted with the subscript 0 in this section) must be renormalized. The renormalized SM masses are defined by

$$M_V^2 = M_{0,V}^2 - \Pi_{VV}(M_V^2), \tag{12}$$

where $\Pi_{VV}(M_V^2)$ is the one-loop correction to the two-point function for Z or W computed on shell. The gauge boson two-point functions in the SMEFT can be found analytically in Refs. [9,26].

The one-loop relation between the VEV and the Fermi constant is

$$G_\mu + \frac{\mathcal{C}_{ll}}{\sqrt{2}\Lambda^2} - \sqrt{2}\frac{\mathcal{C}_{\phi l}^{(3)}}{\Lambda^2} \equiv \frac{1}{\sqrt{2}v_0^2}(1+\Delta r), \tag{13}$$

where v_0 is the unrenormalized minimum of the potential and Δr is obtained from the one-loop corrections to μ decay. Analytic expressions for Δr in both the SM and the SMEFT at dimension 6 are given in Ref. [15].

The calculation proceeds in the same way as Ref. [15]. We obtain the relevant amplitudes using FeynArts [27] with a model file generated by FeynRules [28] with the Feynman rules presented in [21]. Then we use FeynCalc [29,30] to manipulate and reduce the integrals and LoopTools [31] for the numerical evaluation.

We consider two choices of input parameters. For the W^+W^- calculation, we choose the G_μ scheme, where we take the physical input parameters to be[3]

$$G_\mu = 1.1663787(6)\times 10^{-5}\ \text{GeV}^{-2}$$
$$M_Z = 91.1876 \pm .0021\ \text{GeV}$$
$$M_W = 80.385 \pm .015\ \text{GeV}$$
$$M_H = 125.09 \pm 0.21 \pm 0.11\ \text{GeV}$$
$$M_t = 173.1 \pm 0.6\ \text{GeV}.$$

We then follow the same procedure as in Ref. [15]. In our discussion, we term this the "G_μ, M_W, M_Z scheme."

For the decay $H \to \gamma\gamma$, we consider the effects of explicitly pulling out an overall factor of α from the amplitudes; that is, we calculate

$$\mathcal{A}(H \to \gamma\gamma) = \alpha_0 \hat{F}(v_0, M_{0,W}, M_{0,Z}), \tag{14}$$

where F is a function of the bare parameters v_0, $M_{0,W}$, $M_{0,Z}$, that we renormalize as described before and express in terms of G_μ, M_W and M_Z. The on-shell renormalization of the overall factor α is extracted from the renormalization of the $\gamma\bar{l}l$ vertex and we take the physical parameter

$$\alpha = \frac{1}{137.035999139(31)}. \tag{15}$$

We term this the "α, G_μ, M_W, M_Z scheme."

[3]The light quark masses and lepton masses enter into the γ wave-function renormalization for $H \to \gamma\gamma$ and we take $m_b = 4.78$ GeV, $m_c = 1.67$ GeV, $m_s = 0.1$ GeV, $m_d = 0.005$ GeV, $m_u = 0.002$ GeV, $m_\tau = 1.776$ GeV, $m_\mu = 0.105$ GeV and $m_e = 0.0005$ GeV.

III. $H \to W^+W^-$

The tree level decay width for $H \to W^+W^-$ receives contributions from the rescaling of the Higgs field [Eq. (5)], the SMEFT contributions to G_μ [Eq. (9)] and the direct interaction of $O_{\phi W}$. For $M_H = 200$ GeV, the numerical result SMEFT tree level result in GeV is

$$\Gamma_0(H \to W^+W^-) = 1.042 + \left(\frac{1\text{ TeV}}{\Lambda}\right)^2\left\{0.1263\left(\mathcal{C}_{\phi\Box} - \mathcal{C}_{\phi l}^{(3)} - \frac{1}{4}C_{\phi D}\right) - 0.2485(\mathcal{C}_{\phi W} - 0.2541\mathcal{C}_{ll})\right\}$$
$$+ \left(\frac{1\text{ TeV}}{\Lambda}\right)^4\left\{0.003828\left(\mathcal{C}_{\phi\Box} - \mathcal{C}_{\phi l}^{(3)} - \frac{1}{4}C_{\phi D}\right)^2 - 0.01506(\mathcal{C}_{\phi W} - .2541\mathcal{C}_{ll})\left(\mathcal{C}_{\phi\Box} - \mathcal{C}_{\phi l}^{(3)} - \frac{1}{4}\mathcal{C}_{\phi D}\right)\right.$$
$$\left. + 0.02343\mathcal{C}_{\phi W}^2 - 0.007531\mathcal{C}_{\phi W}\mathcal{C}_{ll} + 0.0009570\mathcal{C}_{ll}^2\right\}. \quad (16)$$

We have retained terms of $\mathcal{O}(\mathcal{C}_i^2)$ in Eq. (16) although the numerical coefficients are suppressed relative to those of the $\mathcal{O}(\mathcal{C}_i)$ terms. The usual tree level scaling factor is defined to $\mathcal{O}(\frac{1}{\Lambda^2})$:

$$\mu_0(H \to W^+W^-) = \frac{\Gamma_0(H \to W^+W^-)}{\Gamma_0(H \to W^+W^-)|_{\rm SM}} \to 1.0 + \left(\frac{1\text{ TeV}}{\Lambda}\right)^2\left\{0.1212\left(\mathcal{C}_{\phi\Box} - \mathcal{C}_{\phi l}^{(3)} - \frac{1}{4}\mathcal{C}_{\phi D}\right)\right.$$
$$\left. - 0.2385\mathcal{C}_{\phi W} + 0.06060\mathcal{C}_{ll}\right\}, \quad \text{for } M_H = 200\text{ GeV}. \quad (17)$$

At NLO in the SMEFT, the decay width receives contributions from the one-loop virtual diagrams, including the renormalization terms discussed in the previous section, and from real photon emission. These contributions are separately IR divergent and we regulate them with a photon mass. The SM rate including all electroweak corrections is well known, both for the on-shell decay $H \to W^+W^-$ [32] and the off-shell decays, $H \to 4$ fermions [33]. The off-shell effects are known to be significant for the physical $M_H = 125$ GeV Higgs and the extension of our calculation to include the off-shell effects is clearly a needed step. The SM electroweak corrections are of order ~6% for our reference Higgs mass, $M_H = 200$ GeV.

The calculation of the virtual contribution in the SMEFT follows the identical procedure as for $H \to ZZ$, with the exception of the introduction of a finite photon mass. The renormalization prescription is described in the previous section.

The IR divergences from the virtual diagrams are canceled by real photon emission contributions, $H \to WW\gamma$. Due to the complex Lorentz structures of the SMEFT vertices, the calculation of the width $H \to WW\gamma$ through direct integration of the phase space is extremely intricate. In order to calculate the real corrections we used the method developed in [18], where the integration over the phase space is replaced with a loop integration. This is possible after we recognize that the Cutkosky rules allow us to replace the delta functions inside the phase space integrations with propagators:

$$2i\pi\delta(p^2 - m^2) = \frac{1}{p^2 - m^2 + i0} - \frac{1}{p^2 - m^2 - i0}. \quad (18)$$

After making this replacement, we can treat the momenta of the outgoing particles as internal loop momenta, and the integration over the phase space becomes an integration over the loop momenta. This allow us to use the integration by parts relations to reduce the loop integrals in terms of master integrals (MI). The methodology of this approach is described in Ref. [18].

In the specific case of $H \to WW\gamma$, the integrals obtained are two-point two-loop integrals, for which a generic basis of MI is known [34,35]. The reduction was done using FIRE [36]. Since many two-point two-loop MI are known analytically, and the rest can be calculated numerically with high precision, for example using TSIL [37], we evaluate the MI directly and take the imaginary part of the result. An important caveat is that after the reduction to MI, we have to select only the MI that still have a physical $WW\gamma$ cut, while we put to zero those that have lost one or more of the propagators generated by Eq. (18). An interesting consequence of this is that if an integral can be cut in more than one way it is necessary to add a counterterm to cancel the extra imaginary part. As an example of this procedure, see Fig. 1.

We have verified analytically that the IR divergences proportional to the photon mass cancel using this technique.

The total width is then the sum of the virtual and real contributions, and it is given for $M_H = 200$ GeV by $\Gamma = \Gamma_0 + \delta\Gamma_{\rm NLO}$ with

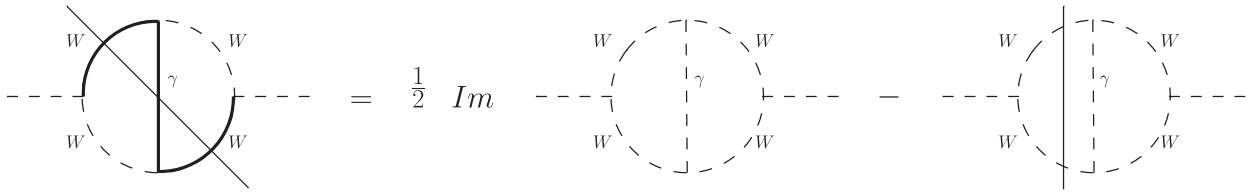

FIG. 1. Example of the calculation of $WW\gamma$ phase space. From the reduction we obtain the central integral. There are four possible ways to cut it: two over WW and two over $WW\gamma$. Since we are interested in calculating the integral with a single physical cut over $WW\gamma$ (left integral), we need to subtract a counterterm (right integral).

$$\begin{aligned}\delta\Gamma_{\rm NLO} = 0.065253 + \left(\frac{1\ {\rm TeV}}{\Lambda}\right)^2 \{&[(190.1 - 70.52X_\Lambda)\mathcal{C}_{\phi\Box}(\Lambda) + (-203.1 + 6.668X_\Lambda)\mathcal{C}^{(3)}_{\phi l}(\Lambda) + (-44.44 + 16.82X_\Lambda)\mathcal{C}_{\phi D}(\Lambda)\\ &+ (-241.4 + 44.54X_\Lambda)\mathcal{C}_{\phi W}(\Lambda) + (71.80 - 3.291X_\Lambda)\mathcal{C}_{ll}(\Lambda)] + (52.06 - 30.64X_\Lambda)\mathcal{C}_{uW}(\Lambda)\\ &+ (-101.0 + 50.69X_\Lambda)\mathcal{C}^{(3)}_{\phi q}(\Lambda) - (5.191 + 32.85X_\Lambda)\mathcal{C}_W(\Lambda) + \mathcal{C}^{(3)}_{lq}(\Lambda)(18.54 - 23.72X_\Lambda)\\ &- 8.434\mathcal{C}_\phi(\Lambda) - 1.157\mathcal{C}_{u\phi}(\Lambda) + (-0.9828 + 2.192X_\Lambda)\mathcal{C}_{\phi B}(\Lambda) + (-17.24 + 3.256X_\Lambda)\mathcal{C}_{\phi WB}(\Lambda)\\ &- 1.290\mathcal{C}^{(1)}_{\phi l}(\Lambda)\} \times 10^{-4},\end{aligned} \tag{19}$$

where the coefficients are evaluated at the scale Λ and $X_\Lambda = \log(\Lambda^2/M_Z^2)$. (The terms in the square brackets occur at tree level.)

We define the (on-shell) scaling factor at one loop for $M_H = 200$ GeV and $\Lambda = 1$ TeV,

$$\begin{aligned}\mu_1(H \to WW) = \frac{\Gamma_0 + \delta\Gamma_{\rm NLO}}{(\Gamma_0 + \delta\Gamma_{\rm NLO})|_{\rm SM}} = 1 + &[0.1007\mathcal{C}_{\phi\Box}(\Lambda) - 0.1295\mathcal{C}^{(3)}_{\phi l}(\Lambda) - 0.02525\mathcal{C}_{\phi D}(\Lambda) - 0.2269\mathcal{C}_{\phi W}(\Lambda)\\ &+ 0.06209\mathcal{C}_{ll(\Lambda)}] + \{-85.64\mathcal{C}_{uW}(\Lambda) + 128.2\mathcal{C}^{(3)}_{\phi q}(\Lambda) - 146.9\mathcal{C}_W(\Lambda)\\ &- 85.94\mathcal{C}^{(3)}_{lq} + -7.617\mathcal{C}_\phi(\Lambda) - 1.04493\mathcal{C}_{u\phi}(\Lambda) + 8.604C_{\phi B}(\Lambda)\\ &- 1.474\mathcal{C}_{\phi WB}(\Lambda) - 1.165\mathcal{C}^{(1)}_{\phi l}(\Lambda)\} \times 10^{-4}.\end{aligned} \tag{20}$$

The change in the coefficients of operators that appear at tree level [in the square brackets in Eq. (20)] is typically a few percent, while a few of the operators that first appear at one loop have sizable coefficients and could potentially be probed in $H \to W^+W-$ decays.

IV. $H \to \gamma\gamma$

As a by-product of our calculation of $H \to ZZ$ and $H \to Z\gamma$ [15], we obtain the SMEFT result for $H \to \gamma^\mu(p_1)\gamma^\nu(p_2)$ at one loop. Gauge invariance requires that the one-loop amplitude take the form

$$\mathcal{A}^{\mu\nu} = F\left(g^{\mu\nu} - \frac{p_1^\nu p_2^\mu}{p_1 \cdot p_2}\right) = (F^0_{\rm SMEFT} + F^1_{\rm SM} + F^1_{\rm SMEFT})\left(g^{\mu\nu} - \frac{p_1^\nu p_2^\mu}{p_1 \cdot p_2}\right), \tag{21}$$

where we have broken up the coefficient into the tree level SMEFT piece, $F^0_{\rm SMEFT}$; the one-loop SM piece, $F^1_{\rm SM}$; and the one-loop SMEFT contribution, $F^1_{\rm SMEFT}$.

Initially, we take M_W, M_Z and G_μ as input parameters. At tree level, there is only the SMEFT contribution,

$$F^0_{\rm SMEFT} = -8M_H^2\frac{M_W^2}{\Lambda^2}\sqrt{\sqrt{2}G_\mu}\left(1 - \frac{M_W^2}{M_Z^2}\right)\mathcal{C}_{\gamma\gamma} \tag{22}$$

where

$$\mathcal{C}_{\gamma\gamma} \equiv \frac{1}{4\sqrt{2}G_\mu M_W^2}\left(\mathcal{C}_{\phi W} + \frac{M_W^2}{M_Z^2 - M_W^2}\mathcal{C}_{\phi B} - \frac{M_W}{\sqrt{M_Z^2 - M_W^2}}\mathcal{C}_{\phi WB}\right). \tag{23}$$

The analytic one-loop SM result can be found in many places [38] and we write the results numerically. The SMEFT logarithms contributing to $F^1_{\rm SMEFT}$ can be obtained from the anomalous dimensions given in Ref. [22] and are written in terms of

$$X_\Lambda = \log\left(\frac{\Lambda^2}{M_Z^2}\right). \tag{24}$$

The full one-loop SMEFT result for $H \to \gamma\gamma$ is extracted from the calculation of Ref. [15] [for the input parameters of Eq. (14)]. Our complete result is

- G_μ, M_W, M_Z input parameter scheme:

$$\begin{aligned}
F^0_{\rm SMEFT} &= \left(\frac{1\ \text{TeV}}{\Lambda}\right)^2\{-5.988\mathcal{C}_{\phi B}(\Lambda) - 1.718\mathcal{C}_{\phi W}(\Lambda) + 3.207\mathcal{C}_{\phi WB}(\Lambda)\}\\
F^1_{\rm SM} &= 0.2483\\
F^1_{\rm SMEFT} &= \left(\frac{1\ \text{TeV}}{\Lambda}\right)^2\{[(0.3636 + 0.1336X_\Lambda)\mathcal{C}_{\phi B}(\Lambda) + (0.02362 + 0.01456X_\Lambda)\mathcal{C}_{\phi W}(\Lambda)\\
&\quad + (-0.1272 - 0.06487X_\Lambda)\mathcal{C}_{\phi WB}(\Lambda)]\\
&\quad + (0.01304 - 0.02725X_\Lambda)\mathcal{C}_W(\Lambda) + 0.01505\mathcal{C}_{\phi\Box}(\Lambda) - 0.03000\mathcal{C}_{\phi D}(\Lambda)\\
&\quad + 0.004279\mathcal{C}_{u\phi}(\Lambda) + (0.1276 - 0.05649X_\Lambda)\mathcal{C}_{uW}(\Lambda) + (0.2383 - 0.1055X_\Lambda)\mathcal{C}_{uB}(\Lambda)\\
&\quad - 0.04516\mathcal{C}^{(3)}_{\phi l}(\Lambda) + 0.02258\mathcal{C}_{ll}(\Lambda)\}.
\end{aligned} \tag{25}$$

The coefficients are given in GeV and are evaluated at the scale Λ. This is the appropriate scale for matching with high-scale UV complete models [39–42]. However, it should be highlighted that in order to be consistent, the matching with the UV model should be computed at NLO. Moreover a more general calculation would require the computation of the RG evolution of the coefficients also at NLO order. This is particularly true when the separation between the electroweak and the EFT scales is very large and it becomes necessary to resum the logarithms $\log(\Lambda^2/M_Z^2)$. Our calculation is a first step in this program. Note the dependence at one loop on coefficients that do not appear at tree level, leading to the interesting possibility of obtaining limits on previously unconstrained coefficients.

We recalculate the result using α, G_μ, M_Z, and M_W as inputs, as described in Sec. II. For notational convenience, the amplitude is expressed as

$$\mathcal{A}^{\mu\nu} = \alpha(\hat{F}^0_{\rm SMEFT} + \hat{F}^1_{\rm SM} + \hat{F}^1_{\rm SMEFT})\left(g^{\mu\nu} - \frac{p_1^\nu p_2^\mu}{p_1\cdot p_2}\right). \tag{26}$$

The result is

- α, G_μ, M_Z, M_W input parameter scheme:

$$\begin{aligned}
\alpha\hat{F}^0_{\rm SMEFT} &= \left(\frac{1\ \text{TeV}}{\Lambda}\right)^2\{-5.778\mathcal{C}_{\phi B}(\Lambda) - 1.657\mathcal{C}_{\phi W}(\Lambda) + 3.095\mathcal{C}_{\phi WB}(\Lambda)\}\\
\alpha\hat{F}^1_{\rm SM} &= 0.2396\\
\alpha\hat{F}^1_{\rm SMEFT} &= \left(\frac{1\ \text{TeV}}{\Lambda}\right)^2\{[(0.1234 + 0.1290X_\Lambda)\mathcal{C}_{\phi B}(\Lambda) + (-0.04246 + 0.01405X_\Lambda)\mathcal{C}_{\phi W}(\Lambda)\\
&\quad + (0.05329 - 0.06260X_\Lambda)\mathcal{C}_{\phi WB}(\Lambda)]\\
&\quad + (0.01259 - 0.02630X_\Lambda)\mathcal{C}_W(\Lambda) + 0.01452\mathcal{C}_{\phi\Box}(\Lambda) - 0.003631\mathcal{C}_{\phi D}(\Lambda)\\
&\quad + 0.004129\mathcal{C}_{u\phi}(\Lambda) + (0.1231 - 0.05451X_\Lambda)\mathcal{C}_{uW}(\Lambda) + (0.2299 - 0.1018X_\Lambda)\mathcal{C}_{uB}(\Lambda)\\
&\quad - 0.01452\mathcal{C}^{(3)}_{\phi l}(\Lambda) + 0.007262\mathcal{C}_{ll}(\Lambda)\}.
\end{aligned} \tag{27}$$

We find that the coefficients calculated in the α, G_μ, M_Z, M_W scheme are in agreement with those calculated in [14]. We also note that in both input schemes, typically the coefficients of the logarithms are of similar sizes to the constant pieces and that the differences are small in most cases. There are, however, a few coefficients where the effect of the choice of the input parameter scheme is significant: comparing Eqs. (25) and (27) one can notice a factor ∼3 between the coefficients of $(\mathcal{C}_{ll} - 2\mathcal{C}_{\phi l}^{(3)})$ and a factor ∼8 between the coefficients of $\mathcal{C}_{\phi D}$. In particular, while $\mathcal{C}_{\phi\Box}$ and $\mathcal{C}_{\phi D}$ appear in Eq. (27) in the combination $(\mathcal{C}_{\phi\Box} - \frac{1}{4}\mathcal{C}_{\phi D})$ that is connected to the redefinition of the Higgs field in Eq. (5), in Eq. (25) one can verify that this simple relation is spoiled and the coefficients appear in the combination $(\mathcal{C}_{\phi\Box} - \frac{M_W^2+M_Z^2}{4(M_Z^2-M_W^2)}\mathcal{C}_{\phi D}) \sim (\mathcal{C}_{\phi\Box} - 2\mathcal{C}_{\phi D})$. These differences are due to the fact that using α, G_μ, M_Z, and M_W as input parameters modifies the counting of $\mathcal{C}_{\phi D}$ and $(\mathcal{C}_{ll} - 2\mathcal{C}_{\phi l}^{(3)})$ that enter in the relation between the Lagrangian parameters and the input parameters α and G_μ respectively [see Eqs. (3.4)–(3.6) and (3.20) of [43], for example]. Notice that the change of input parameter scheme affects also the coefficient of $\mathcal{C}_{\phi WB}$ that is present in the relation between the Lagrangian parameters and α. However this effect is hidden in the relation between Eqs. (25) and (27) by the fact that $\mathcal{C}_{\phi WB}$ appears already at the LO with a large coefficient. The effect is instead evident in Eqs. (A1) and (A2) in the Appendix, where $\mathcal{C}_{\phi WB}$ appears only at the NLO. The loop corrections to $C_{\phi W}$, $C_{\phi B}$ and $C_{\phi WB}$ are on the order of 1%–2%, relative to the tree level results.

We study the numerical consequences of our calculations by considering[4]

$$\begin{aligned}\mu_{\gamma\gamma} &\equiv \frac{\Gamma(H\to\gamma\gamma)}{\Gamma(H\to\gamma\gamma)_{SM}} \\ &= 1 + \frac{2(F^0_{\rm SMEFT} + F^1_{\rm SMEFT})}{F^1_{SM}} + \mathcal{O}\left(\frac{1}{\Lambda^4}\right) \\ &= 1 + [-40.15\mathcal{C}_{\phi B}(\Lambda) - 13.08\mathcal{C}_{\phi W}(\Lambda) \\ &\quad + 22.40\mathcal{C}_{\phi WB}(\Lambda)] - 0.9463\mathcal{C}_W(\Lambda) + 0.1212\mathcal{C}_{\phi\Box}(\Lambda) \\ &\quad - 0.2417\mathcal{C}_{\phi D}(\Lambda) + 0.03447\mathcal{C}_{u\phi}(\Lambda) - 1.151\mathcal{C}_{uW}(\Lambda) \\ &\quad - 2.150\mathcal{C}_{uB}(\Lambda) - 0.3637\mathcal{C}_{\phi l}^{(3)}(\Lambda) + 0.1819\mathcal{C}_{ll}(\Lambda).\end{aligned} \tag{28}$$

Our results can be compared with the limits from ATLAS [4,44] and CMS [4,45]:

[4]Equation (28) is in the G_μ, M_Z, M_W scheme.

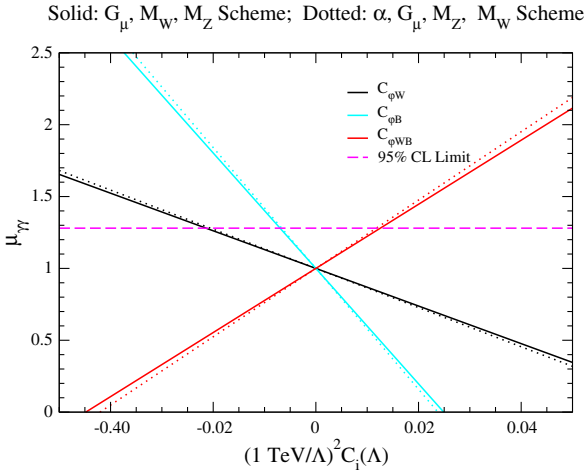

FIG. 2. Contributions to $\mu_{\gamma\gamma}$ when one operator at a time is varied, setting the remaining operators to 0. The coefficients are evaluated at the scale $\Lambda = 1$ TeV.

$$\begin{aligned}\text{ATLAS, Run}-2&:\ \mu_{\gamma\gamma} = 0.99 \pm 0.15 \\ \text{ATLAS, Run}-1&:\ \mu_{\gamma\gamma} = 1.14 \pm 0.27 \\ \text{CMS, Run}-2&:\ \mu_{\gamma\gamma} = 1.18 \pm 0.17 \\ \text{CMS, Run}-1&:\ \mu_{\gamma\gamma} = 1.11 \pm 0.25.\end{aligned} \tag{29}$$

We make the simplifying assumption that there are no cancellations between terms and require that no single contribution saturate the experimental bound. This is probably a poor assumption, since in any specific model, there are relations between the SMEFT coefficients [40,41,46]. When the complete set of one-loop SMEFT predictions to Higgs decay is known, it will be possible to do a global fit incorporating these effects. In extracting the bounds, we are also ignoring the NLO effects induced by the matching with a UV theory, and the RG evolution discussed at the beginning of this session. A full NLO RGE calculation would be needed in order to reliably understand the size of these effects. Our bounds are therefore only rough estimates of the sensitivity. In Fig. 2 we show the bounds on the coefficients that occur at tree level. The argument of the logarithms is evaluated at $\Lambda = 1$ TeV. The solid lines are the contributions in the G_μ, M_Z, M_W scheme and the dotted lines are the G_μ, M_Z, M_W, α scheme. Requiring that $0 < \mu_{\gamma\gamma} < 1.28$, we find for $\Lambda = 1$ TeV[5]

$$\begin{aligned}|\mathcal{C}_{\phi W}(\Lambda)| &< 0.02 \\ |\mathcal{C}_{\phi B}(\Lambda)| &< 0.001 \quad (H\to\gamma\gamma \text{ limit}) \\ |\mathcal{C}_{\phi WB}(\Lambda)| &< 0.01.\end{aligned} \tag{30}$$

[5]Reference [14] requires $0.85 < \mu_{\gamma\gamma} < 1.15$ and so finds somewhat more restrictive limits. The coefficients in Ref. [14] are evaluated at the scale $\mu = M_W$.

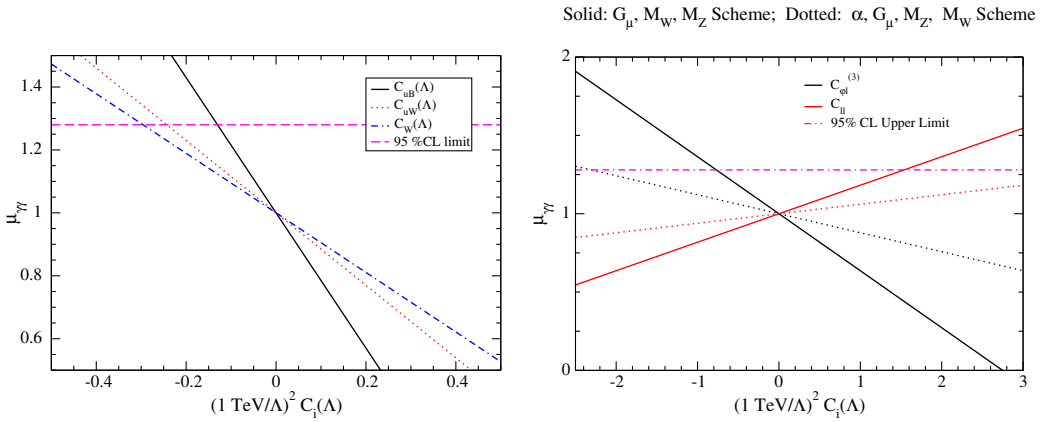

FIG. 3. Contributions to $\mu_{\gamma\gamma}$ when one operator at a time is varied, setting the remaining operators to 0. The coefficients are evaluated at the scale $\Lambda = 1$ TeV. On the left hand side, the solid and dotted lines are indistinguishable.

The coefficients can be evolved to low scales, $\mu \sim M_Z$, using the anomalous dimension matrix,

$$\mathcal{C}_i(M_Z) = \mathcal{C}_i(\Lambda) - \frac{\gamma_{ij}\mathcal{C}_j}{16\pi^2}\log\left(\frac{\Lambda}{M_Z}\right), \tag{31}$$

where the anomalous dimension matrices can be found in Refs. [22] and the analogous numerical result to Eq. (28), but with the coefficients evaluated at a low scale, can be found in Ref. [14].

On the left hand side of Fig. 3 we show the contributions to $\mu_{\gamma\gamma}$ from $\mathcal{C}_{uB}$ and $\mathcal{C}_{uW}$. These coefficients first appear at loop level and it is interesting that $H \to \gamma\gamma$ has the potential to place limits on them. We find (for $\Lambda = 1$ TeV)

$$\begin{aligned} |\mathcal{C}_{uB}(\Lambda)| &< 0.14 \quad (H \to \gamma\gamma \text{ limit}) \\ |\mathcal{C}_{uW}(\Lambda)| &< 0.23. \end{aligned} \tag{32}$$

The contribution from $\mathcal{C}_W$ is shown on the left hand side of Fig. 3. This operator is particularly interesting because it contributes to W^+W^- pair production [47,48]. Translating the tree level results of Ref. [49] into our notation, we have for $\Lambda = 1$ TeV

$$|\mathcal{C}_W| < 0.08 \quad (W^+W^- \text{ limit}). \tag{33}$$

From Fig. 3, the limit on $\mathcal{C}_W$ from $H \to \gamma\gamma$ assuming that $\mathcal{C}_W$ is the only nonzero coefficient is $|\mathcal{C}_W| < 0.3$, significantly weaker than the limit from gauge boson pair production.

The contributions of $\mathcal{C}_{\phi l}^{(3)}$ and $\mathcal{C}_{ll}$ are particularly interesting because they contribute to G_μ at tree level and are shown on the right hand side of Fig. 3. From Eq. (9), they always contribute in the combination $\mathcal{C}_{\phi l}^{(3)} - \frac{1}{2}\mathcal{C}_{ll}$. The overall numerical factor between the schemes is just the difference in input parameters.

V. CONCLUSIONS

We have computed the one-loop electroweak corrections to the decays $H \to \gamma\gamma$ and $H \to W^+W^-$ in the SMEFT. The results are presented in simple forms, useful for comparison with LHC data and for matching with the predictions of UV complete theories.

The decay $H \to \gamma\gamma$ is found using two different input parameter schemes and the numerical dependence on the scheme choice is negligible except for the coefficients of the operators $O_{\phi l}^{(3)}$ and O_{ll} that contribute to G_μ at tree level. For operators that contribute to $H \to \gamma\gamma$ at tree level, the effect of the NLO corrections is a few percent. However, the NLO result offers the possibility of constraining operators that first appear at one loop.

The real corrections to the on-shell decay $H \to W^+W^-\gamma$ are determined by transforming the three-body final state phase space into two-loop integrals, while the virtual corrections are obtained using standard techniques. The relatively large size of some of the one-loop contributions suggests that a complete calculation of the off-shell decay $H \to 4$ fermions at one loop in the SMEFT is of interest.

ACKNOWLEDGMENTS

We thank Ahmed Ismail for discussions. We thank Athanasios Dedes and Michalis Paraskevas for comments on the first version this paper. S. D. and P. P. G are supported by the U.S. Department of Energy under Contract No. de-sc0012704.

APPENDIX: RESULTS IN TERMS OF $\mathcal{C}_{\gamma\gamma}$

It is interesting to replace $\mathcal{C}_{\phi B}$ with $\mathcal{C}_{\gamma\gamma}$. Note that the tree level relation of Eq. (23) cannot be used, but we need the full one-loop calculation for consistency. The results in GeV with $\Lambda = 1$ TeV are

• G_μ, M_W, M_Z input parameter scheme:

$$
\begin{aligned}
F^0_{\mathrm{SMEFT}} &= -0.73\left(\frac{1\ \mathrm{TeV}}{\Lambda}\right)^2 \mathcal{C}_{\gamma\gamma}(\Lambda) \\
F^1_{\mathrm{SM}} &= 0.2483 \\
F^1_{\mathrm{SMEFT}} &= \left(\frac{1\ \mathrm{TeV}}{\Lambda}\right)^2 \{(0.009007 + 0.01247X_\Lambda)\mathcal{C}_{\gamma\gamma}(\Lambda) - (0.01904 + 0.01549X_\Lambda)\mathcal{C}_{\phi WB}(\Lambda) \\
&\quad + (0.01304 - 0.02725X_\Lambda)\mathcal{C}_W(\Lambda) + 0.01505\mathcal{C}_{\phi\Box}(\Lambda) - 0.03000\mathcal{C}_{\phi D}(\Lambda) + 0.004279\mathcal{C}_{u\phi}(\Lambda) \\
&\quad + 0.01203\mathcal{C}_{\phi W}(\Lambda) + (0.1276 - 0.05649X_\Lambda)\mathcal{C}_{uW}(\Lambda) + (0.2383 - 0.1055X_\Lambda)\mathcal{C}_{uB}(\Lambda) \\
&\quad - 0.04516\mathcal{C}^{(3)}_{\phi l}(\Lambda) + 0.02258\mathcal{C}_{ll}(\Lambda)\}
\end{aligned}
\tag{A1}
$$

• α, G_μ, M_Z, M_W input parameter scheme:
The coefficients are

$$
\begin{aligned}
\alpha\hat{F}^0_{\mathrm{SMEFT}} &= -\left(\frac{1\ \mathrm{TeV}}{\Lambda}\right)^2 0.7066\mathcal{C}_{\gamma\gamma}(\Lambda) \\
\alpha\hat{F}^1_{\mathrm{SM}} &= 0.2396 \\
\alpha\hat{F}^1_{\mathrm{SMEFT}} &= \left(\frac{1\ \mathrm{TeV}}{\Lambda}\right)^2 \{(-0.01913 + 0.01203X_\Lambda)\mathcal{C}_{\gamma\gamma}(\Lambda) + (0.03587 - 0.01495X_\Lambda)\mathcal{C}_{\phi WB}(\Lambda) \\
&\quad + (0.01259 - 0.02630X_\Lambda)\mathcal{C}_W(\Lambda) + 0.01452\mathcal{C}_{\phi\Box}(\Lambda) - 0.003631\mathcal{C}_{\phi D}(\Lambda) + 0.004129\mathcal{C}_{u\phi}(\Lambda) \\
&\quad + 0.01161\mathcal{C}_{\phi W}(\Lambda) + (0.1231 - 0.05451X_\Lambda)\mathcal{C}_{uW}(\Lambda) + (0.2299 - 0.1018X_\Lambda)\mathcal{C}_{uB}(\Lambda) \\
&\quad - 0.01452\mathcal{C}^{(3)}_{\phi l}(\Lambda) + 0.007262\mathcal{C}_{ll}(\Lambda)\}.
\end{aligned}
\tag{A2}
$$

[1] CMS Collaboration, Projected performance of Higgs analyses at the HL-LHC for ECFA 2016, CERN Technical Report No. CMS-PAS-FTR-16-002, https://cds.cern.ch/record/2266165.

[2] ATLAS Collaboration, Projections for measurements of Higgs boson cross sections, branching ratios and coupling parameters with the ATLAS detector at a HL-LHC, CERN Technical Report No. ATL-PHYS-PUB-2013-014, 2013, https://cds.cern.ch/record/1611186.

[3] D. de Florian *et al.* (LHC Higgs Cross Section Working Group Collaboration), Handbook of LHC Higgs cross sections: 4. Deciphering the nature of the Higgs sector, arXiv:1610.07922.

[4] G. Aad *et al.* (ATLAS and CMS Collaborations), Measurements of the Higgs boson production and decay rates and constraints on its couplings from a combined ATLAS and CMS analysis of the LHC pp collision data at $\sqrt{s} = 7$ and 8 TeV, J. High Energy Phys. 08 (2016) 045.

[5] G. F. Giudice, C. Grojean, A. Pomarol, and R. Rattazzi, The strongly-interacting light Higgs, J. High Energy Phys. 06 (2007) 045.

[6] I. Brivio and M. Trott, The Standard Model as an effective field theory, arXiv:1706.08945.

[7] R. Contino, M. Ghezzi, C. Grojean, M. Muhlleitner, and M. Spira, eHDECAY: An implementation of the Higgs effective Lagrangian into HDECAY, Comput. Phys. Commun. **185**, 3412 (2014).

[8] J. A. A. Saavedra *et al.*, Interpreting top-quark LHC measurements in the standard-model effective field theory, arXiv:1802.07237.

[9] M. Ghezzi, R. Gomez-Ambrosio, G. Passarino, and S. Uccirati, NLO Higgs effective field theory and κ-framework, J. High Energy Phys. 07 (2015) 175.

[10] R. Gauld, B. D. Pecjak, and D. J. Scott, QCD radiative corrections for $h \to b\bar{b}$ in the Standard Model dimension-6 EFT, Phys. Rev. D **94**, 074045 (2016).

[11] R. Gauld, B. D. Pecjak, and D. J. Scott, One-loop corrections to $h \to b\bar{b}$ and $h \to \tau\bar{\tau}$ decays in the Standard Model dimension-6 EFT: Four-fermion operators and the large-m_t limit, J. High Energy Phys. 05 (2016) 080.

[12] C. Hartmann and M. Trott, Higgs Decay to Two Photons at One Loop in the Standard Model Effective Field Theory, Phys. Rev. Lett. **115**, 191801 (2015).

[13] C. Hartmann and M. Trott, On one-loop corrections in the Standard Model effective field theory; the $\Gamma(h \to \gamma\gamma)$ case, J. High Energy Phys. 07 (2015) 151.
[14] A. Dedes, M. Paraskevas, J. Rosiek, K. Suxho, and L. Trifyllis, The decay $h \to \gamma\gamma$ in the Standard-Model effective field theory, J. High Energy Phys. 08 (2018) 103.
[15] S. Dawson and P. P. Giardino, Higgs decays to ZZ and $Z\gamma$ in the Standard Model effective field theory: An NLO analysis, Phys. Rev. D **97**, 093003(2018).
[16] C. Hartmann, W. Shepherd, and M. Trott, The Z decay width in the SMEFT: y_t and λ corrections at one loop, J. High Energy Phys. 03 (**2017**) 060.
[17] E. Vryonidou and C. Zhang, Dimension-six electroweak top-loop effects in Higgs production and decay, J. High Energy Phys. 08 (2018) 036.
[18] C. Anastasiou and K. Melnikov, Higgs boson production at hadron colliders in NNLO QCD, Nucl. Phys. **B646**, 220 (2002).
[19] W. Buchmuller and D. Wyler, Effective Lagrangian analysis of new interactions and flavor conservation, Nucl. Phys. **B268**, 621 (1986).
[20] B. Grzadkowski, M. Iskrzynski, M. Misiak, and J. Rosiek, Dimension-six terms in the Standard Model Lagrangian, J. High Energy Phys. 10 (**2010**) 085.
[21] A. Dedes, W. Materkowska, M. Paraskevas, J. Rosiek, and K. Suxho, Feynman rules for the Standard Model effective field theory in R_ξ-gauges, J. High Energy Phys. 06 (2017) 143.
[22] R. Alonso, E. E. Jenkins, A. V. Manohar, and M. Trott, Renormalization group evolution of the Standard Model dimension six operators III: Gauge coupling dependence and phenomenology, J. High Energy Phys. 04 (2014) 159.
[23] J. Fleischer and F. Jegerlehner, Radiative corrections to Higgs decays in the extended Weinberg-Salam model, Phys. Rev. D **23**, 2001 (1981).
[24] E. E. Jenkins, A. V. Manohar, and M. Trott, Renormalization group evolution of the Standard Model dimension six operators I: Formalism and lambda dependence, J. High Energy Phys. 10 (2013) 087.
[25] E. E. Jenkins, A. V. Manohar, and M. Trott, Renormalization group evolution of the Standard Model dimension six operators II: Yukawa dependence, J. High Energy Phys. 01 (2014) 035.
[26] C.-Y. Chen, S. Dawson, and C. Zhang, Electroweak effective operators and Higgs physics, Phys. Rev. D **89**, 015016 (2014).
[27] T. Hahn, Generating Feynman diagrams and amplitudes with FeynArts 3, Comput. Phys. Commun. **140**, 418 (2001).
[28] A. Alloul, N. D. Christensen, C. Degrande, C. Duhr, and B. Fuks, FeynRules 2.0 - A complete toolbox for tree-level phenomenology, Comput. Phys. Commun. **185**, 2250 (2014).
[29] R. Mertig, M. Bohm, and A. Denner, FEYN CALC: Computer algebraic calculation of Feynman amplitudes, Comput. Phys. Commun. **64**, 345 (1991).
[30] V. Shtabovenko, R. Mertig, and F. Orellana, New developments in FeynCalc 9.0, Comput. Phys. Commun. **207**, 432 (2016).
[31] T. Hahn, Automatic loop calculations with FeynArts, FormCalc, and LoopTools, Nucl. Phys. B, Proc. Suppl. **89**, 231 (2000).
[32] B. A. Kniehl, Radiative corrections for $H \to W^+W^-$ (γ) in the Standard Model, Nucl. Phys. **B357**, 439 (1991).
[33] A. Bredenstein, A. Denner, S. Dittmaier, and M. M. Weber, Radiative corrections to the semileptonic and hadronic Higgs-boson decays $H \to WW/ZZ \to 4$ fermions, J. High Energy Phys. 02 (2007) 080.
[34] O. V. Tarasov, Generalized recurrence relations for two loop propagator integrals with arbitrary masses, Nucl. Phys. **B502**, 455 (1997).
[35] S. P. Martin, Evaluation of two loop self-energy basis integrals using differential equations, Phys. Rev. D **68**, 075002 (2003).
[36] A. V. Smirnov, FIRE5: A C++ implementation of Feynman Integral REduction, Comput. Phys. Commun. **189**, 182 (2015).
[37] S. P. Martin and D. G. Robertson, TSIL: A program for the calculation of two-loop self-energy integrals, Comput. Phys. Commun. **174**, 133 (2006).
[38] J. R. Ellis, M. K. Gaillard, and D. V. Nanopoulos, A phenomenological profile of the Higgs boson, Nucl. Phys. **B106**, 292 (1976).
[39] J. Brehmer, A. Freitas, D. Lopez-Val, and T. Plehn, Pushing Higgs effective theory to its limits, Phys. Rev. D **93**, 075014 (2016).
[40] S. Dawson and C. W. Murphy, Standard Model EFT and extended scalar sectors, Phys. Rev. D **96**, 015041 (2017).
[41] J. de Blas, J. C. Criado, M. Perez-Victoria, and J. Santiago, Effective description of general extensions of the Standard Model: The complete tree-level dictionary, J. High Energy Phys. 03 (2018) 109.
[42] F. del Aguila, Z. Kunszt, and J. Santiago, One-loop effective Lagrangians after matching, Eur. Phys. J. C **76**, 244 (2016).
[43] I. Brivio and M. Trott, Scheming in the SMEFT… and a reparameterization invariance!, J. High Energy Phys. 07 (2017) 148; Addendum, J. High Energy Phys. 05 (2018) 136(A).
[44] M. Aaboud *et al.* (ATLAS Collaboration), Measurements of Higgs boson properties in the diphoton decay channel with 36 fb^{-1} of pp collision data at $\sqrt{s} = 13$ TeV with the ATLAS detector, Phys. Rev. D **98**, 052005 (2018).
[45] A. M. Sirunyan *et al.* (CMS Collaboration), Measurements of Higgs boson properties in the diphoton decay channel in proton-proton collisions at $\sqrt{s} = 13$ TeV, arXiv: 1804.02716.
[46] B. Henning, X. Lu, and H. Murayama, How to use the Standard Model effective field theory, J. High Energy Phys. 01 (2016) 023.
[47] A. Falkowski and F. Riva, Model-independent precision constraints on dimension-6 operators, J. High Energy Phys. 02 (2015) 039.
[48] J. Baglio, S. Dawson, and I. M. Lewis, An NLO QCD effective field theory analysis of W^+W^- production at the LHC including fermionic operators, Phys. Rev. D **96**, 073003 (2017).
[49] A. Alves, N. Rosa-Agostinho, O. J. P. Eboli, and M. C. Gonzalez-Garcia, Effect of Fermionic operators on the gauge legacy of the LHC Run I, Phys. Rev. D **98**, 013006 (2018).